

# An elastic phenomenological material law for textile composites and it's fitting to experimental data

Dezső Hegyi

*Dept. Mechanics, Materials and Structures, Budapest University of Technology and Economics, Budapest, Hungary*

+36 1 463 2316

+36 1 463 1773

[hegyi.dezso@szt.bme.hu](mailto:hegyi.dezso@szt.bme.hu)

[www.szt.bme.hu](http://www.szt.bme.hu)

Marianna Halász

*Dept. Polymer Engineering, Budapest University of Technology and Economics, Budapest, Hungary*

+36 1 463 2650

[halaszm@pt.bme.hu](mailto:halaszm@pt.bme.hu)

[www.pt.bme.hu](http://www.pt.bme.hu)

Kolos Molnár

*Dept. Polymer Engineering, Budapest University of Technology and Economics, Budapest, Hungary*

+36 1 463 3083

[molnar@pt.bme.hu](mailto:molnar@pt.bme.hu)

[www.pt.bme.hu](http://www.pt.bme.hu)

Gábor Szebenyi

*Dept. Polymer Engineering, Budapest University of Technology and Economics, Budapest, Hungary*

+36 1 463 1466

[szebenyi@pt.bme.hu](mailto:szebenyi@pt.bme.hu)

[www.pt.bme.hu](http://www.pt.bme.hu)

András A. Sipos

*Dept. Mechanics, Materials and Structures, Budapest University of Technology and Economics, Budapest, Hungary*

+36 1 463 2316

[siposa@eik.bme.hu](mailto:siposa@eik.bme.hu)

[www.szt.bme.hu](http://www.szt.bme.hu)

**Abstract** Constitutive description of deformations in technical textiles mostly requires some highly nonlinear material law due to the interaction between the orthotropic yarns and the effect of the matrix. Phenomenological models aim to garb the overall (macro level) behavior required for engineering purposes. This paper introduces a new, two-dimensional phenomenological model for technical textiles accompanied by a data acquiring strategy to determine the material parameters involved in the model. It handles the nonlinear stress-strain relation observed in uniaxial tests and take the interactions in the two, orthogonal directions into account. As we aim to introduce a

solution applicable at the service level of the loads, our model is inherently elastic, no time dependent or plastic behavior are introduced and no cyclic loading is taken into consideration. The model can be solidly fit to the measured data.

*Keywords: technical textiles, biaxial test, nonlinear constitutive law*

## 1. Introduction

The observed deformation of textile composites under in-plane loading is nonlinear for several reasons: geometrical nonlinearity can be associated with the woven microstructure of the textile and the yarns contribute in a significant material nonlinearity. Furthermore - for specific materials - substantial time-dependent deformations may occur. Because of some nonlinear phenomena, namely plastic yield and time-dependent deformation, the cyclic loading exhibit significantly different stress-strain curves compared to the initial deformation.

This paper is intended to describe a data acquiring strategy and a novel nonlinear elastic constitutive model which takes the interaction between the two orthotropic directions into account.

The new phenomenological model aims to provide a fairly accurate method for the structural analysis of textile materials at the service level of the loads. The ultimate failure of the structure is not in our interest. The widely used partial (safety) factors for technical textiles limit the service stress level to 30-40 % of the ultimate strength of the material. To reduce the effect of plasticity and viscous deformations, PTFE coated glass fiber woven textile was used in short-time uniaxial and biaxial tests. In our work we focus on the first loading and exclude cyclic loading. Nevertheless, the new model can be easily applied for data obtained from cyclic measurements.

The glass fiber has an almost linear elastic behavior and essentially no viscous deformation at the targeted (moderate) stress level. Nevertheless, the measured data reflects the nonlinear effect of the PTFE coating.

Recent methods in the literature are based on the adequate involvement of the material's microstructure (Haan et al. 2001, Ballhause et al. 2005, Durville 2005). They construct the model from feasible components at the micro level via detailed constitutive laws of the yarns, the coating matrix and the interactions between these elements. The phenomenological model at the continuum level is reached via some homogenization technique or an appropriate strain-energy function is defined (dell'Isola and Steigman 2015) that adequately describes the behavior of the fabric. Nevertheless, a detailed description of the internal geometry is also essential in this case. A shortcoming of such approaches is the high computational cost arising from the detailed description. Therefore, these methods are most often impractical for engineering problems.

There are phenomenological methods that describe the overall (macro) nonlinear behavior of the continuum by adequate nonlinear functions. Nevertheless, such a non-linear relation can be derived for models based on the microstructure mentioned above. However - as long as the elastic range is treated - a direct fit for macroscopic data might be preferable, since the assessment of numerous material parameters and the detailed geometry (needed for modeling at the fabric level) can

be omitted. Apparently, there are several, solely macroscopic models in the literature. The dense net method uses two independent functions to be fitted to the uniaxial measurements in the two orthotropic directions (Ambroziak and Klosowski 2005, 2014). It uses nonlinear functions to represent the different slopes of the stress-strain curves (Chaboche 1989, Bodner and Partom 1975), however it lacks to handle the interaction between the two orthogonal yarn directions, practically there is no transversal interaction in the model. Spline methods (Day 1986, Bridgens and Gosling 2004, 2005) define the surface for the stress as a function of the two orthogonal elongations. By this method an accurate interpolation can be achieved to the measured data and the transversal interaction is accounted, too. Nevertheless, the usage of the power equations of the spline can lead to divergence in the nonlinear analysis because the power equations are hectic for extrapolation. During the nonlinear analysis of membrane extremely high strains occur, thus unreliable extrapolation should be avoided.

Our approach can be interpreted as a generalization of the classical elastic constitutive law for an orthotropic medium in two dimensions (Lampiere 1968, Sipos and Fehér 2016). To provide a better fit with the measured data in uniaxial and biaxial tests, exponential functions are used and the interaction of the two directions is modeled with a power function. The new elastic model gives a good approximation at the service load level of the structure for the initial deformations and presents a proper extrapolation to have a stable numerical analysis. This is necessary to avoid the instability in the numerical analysis of the structure at stress localization zones (Sadd 2009).

## **2. Model development**

The technical textiles are built of woven fibers covered by matrix. The present paper use the experimental data measured on glass fiber covered PTFE. The specific material was made by simple chain woven technic.

The fibers inside the textile form a complex 3D geometry. The interaction between the fibers represent highly nonlinear stress-strain function even if the original fiber was almost linear elastic. The initially curved and slack fibers under stress become more strait and taut and stiff. The stress-strain diagram become steep after a moderate slant initial period (Fig. 1. and 2.).

Our goal is to develop a phenomenology model represent the material behavior above.

### **2.1. Uniaxial behavior**

A realistic model should simultaneously explain the material response in uniaxial and biaxial tests. First, we introduce the terms reproducing the uniaxial behavior. Nevertheless, the uniaxial response is tested in the wrap and weft directions separately. Two typical uniaxial tensile test curves are depicted in Fig. 1 and Fig. 2 in the warp and in the weft directions, respectively (These curves are parts of the series of the measurements described in Section 3 in detail. All parameters of the material and the measurement method is described there.).

In all measurements, we determine the engineering stress: the strain is related to the original length and the stress is calculated by the original area of the cross

section. In nonlinear calculations usually the Lagrange strain is used with the Second-Piola stress tensor to model large strains. In the case of membrane structures higher accuracy is required: the Biot strain and Cauchy stress tensors are practical (Hegyi et al. 2005, Hegyi 2006). However, the Biot strain is practically identical to the stretch tensor; we take advantage of this observation in the parameter analysis. During the analysis of the experimental data the stretch and the engineering stress can be easily calculated.

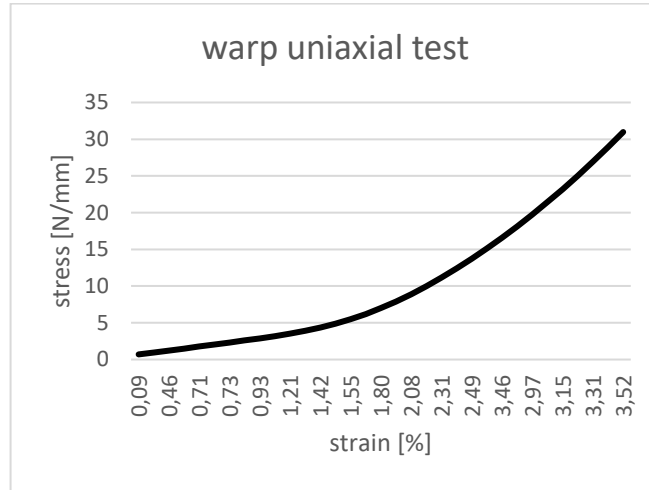


Figure 1. Measured stress, a typical stress-strain curve of a uniaxial tensile test in the warp direction.

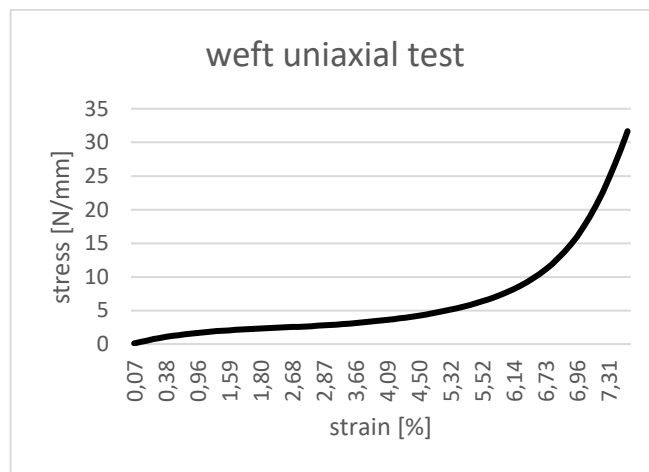


Figure 2. Measured stress, a typical stress-strain curve of a uniaxial tensile test in the weft direction

It is worthy to note, that the stress-strain curves above hints to an inflection point along the curve. This feature seems to be typical among technical textiles. To reproduce the inflection in the uniaxial response a reasonable choice is a linear combination of two exponentials:

$$\sigma_{w,0} = f_{x1}(\varepsilon_w) + f_{x2}(\varepsilon_w) = a_1 \varepsilon_w (1 - e^{-a_3 \varepsilon_w^2}) + a_2 \varepsilon_w (e^{-a_4 \varepsilon_w^2}), \quad (1)$$

$$\sigma_{f,0} = f_{y1}(\varepsilon_f) + f_{y2}(\varepsilon_f) = b_1 \varepsilon_f (1 - e^{-b_3 \varepsilon_f^2}) + b_2 \varepsilon_f (e^{-b_4 \varepsilon_f^2}) \quad (2)$$

where  $\sigma_{w,0}$  [N/mm] is the stress in the warp direction,  $\varepsilon_w$  [%] is the strain in the warp direction and  $a_1, a_2, a_3$  and  $a_4$  are material parameters, where  $a_3$  and  $a_4$  are dimensionless and  $a_1$  and  $a_2$  are in [N/mm] Similarly,  $\sigma_{f,0}$  and  $\varepsilon_f$  denote the stress and strain in the weft direction, respectively. This expression produces a fair fit to the measured stress-strain diagrams: observe the resemblance of the  $\sigma_w$  curve in Fig. 3 (with parameters  $a_1=2,0 - a_2=0,5 - a_3=0,5 - a_4=10$ ) and the output of the measurements in Figures 1 and 2.

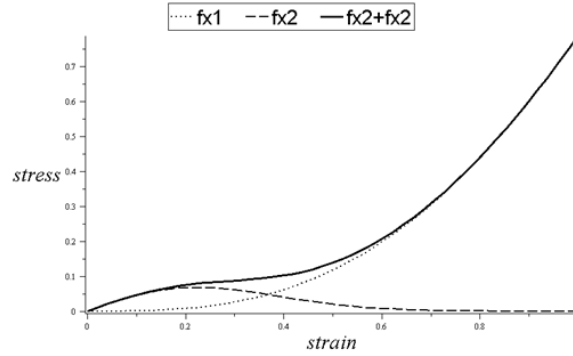


Figure 3. Calculated stress-strain diagram plotted by exponential functions.

## 2.2. Interaction between the two yarn directions

Any elastic constitutive law should satisfy the energy conservation law. It is well known, that this requirement manifests in a symmetric stiffness matrix. In other words, the following derivatives must be equal:

$$\frac{\partial \sigma_w}{\partial \varepsilon_f} = \frac{\partial \sigma_f}{\partial \varepsilon_w} \quad (5)$$

where  $\sigma_w$  and  $\sigma_f$  are the stress in the warp and fill directions, respectively. Nevertheless, in the general case  $\sigma_w$  and  $\sigma_f$  are functions of two variables,  $\varepsilon_w$  and  $\varepsilon_f$ .

We seek a form that satisfy Eq. 5, and that is in accordance with the measured stresses in the biaxial tests and the transversal deformations in the uniaxial tests. This latest is an inherent consequence of the microstructure of the material. In specific, the yarns of textile composites are woven, they mutually bend each other. The matrix (PTFE in our samples) around the yarns are much softer than the yarns itself, thus the matrix contributes to the total deformation, too. This special arrangement has a significant effect on the transversal deformations.

For uniaxial tests Figs. 4 and 5 depict the measured transversal deformation.

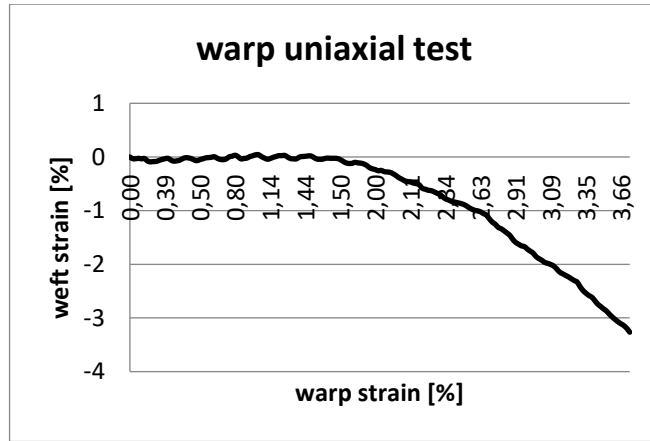


Figure 4. Transversal deformation, uniaxial test, warp loading.

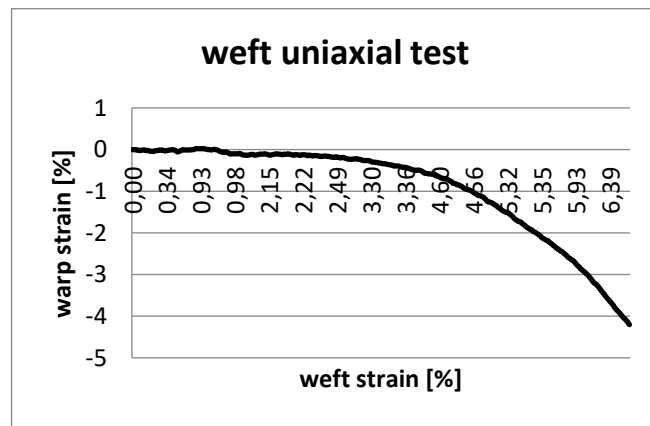


Figure 5. Transversal deformation, uniaxial test, weft loading.

The trend of the transversal deformations in the uniaxial tests (Fig. 4. and 5.) makes it clear that the terms expressing interaction between the two directions cannot be linear. This means, a simple orthotropic response is not sufficient in our case. With a slight generalization of the orthotropic model one arrives to the following expression (it includes the terms from Eqs. (8) and (9)):

$$\sigma_w = a_1 \varepsilon_w (1 - e^{-a_3 \varepsilon_w^2}) + a_2 \varepsilon_w (e^{-a_4 \varepsilon_w^2}) + c_1 \varepsilon_f (\varepsilon_w^2 \varepsilon_f^2)^{c_2}, \quad (8)$$

$$\sigma_f = b_1 \varepsilon_f (1 - e^{-b_3 \varepsilon_f^2}) + b_2 \varepsilon_f (e^{-b_4 \varepsilon_f^2}) + c_1 \varepsilon_w (\varepsilon_w^2 \varepsilon_f^2)^{c_2}. \quad (9)$$

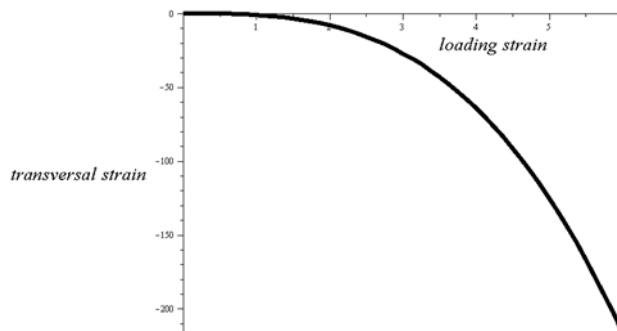


Figure 6. Calculated transversal deformation for uniaxial loading.

Figure 6 represent the calculated curve of the transversal deformation with parameters  $a_1=1, a_2=1, a_3=1, a_4=1, c_1=1, c_2=0,25$ .

Note, that  $c_1$  and  $c_2$  are material parameters. With  $a_1=a_3=a_4=b_1=b_3=b_4=c_2=0$  we obtain the classical linear model of an orthotropic medium. Nevertheless, the symmetry condition in Eq. (5), and thus the energy conservation criteria is satisfied:

$$\frac{\partial \sigma_w}{\partial \sigma_f} = \frac{\partial \sigma_f}{\partial \sigma_w} = 2c_1c_2(\varepsilon_w\varepsilon_f)^{2c_2} + c_1(\varepsilon_w\varepsilon_f)^{2c_2}. \quad (10)$$

Observe the similarity between the measured and computed transversal deformations in Figs. 4, 5 and 6.

A realistic model should contain a contribution from shear. At this stage of model development we neglect that contribution since the shear stiffness of technical textiles is about two order smaller respect to the normal stiffness in one of the orthogonal directions (Day 1986). Based on our experience, just about 1-2% of the initial slope of the normal strain can be used as a good approximation (Hegyí 2006). This observation significantly simplifies the experimental work, too.

Our assumption about the magnitudes of shear has another consequence: we take a nearly diagonal deformation gradient  $\mathbf{F}$  associated with the measurements. The Biot strain in this special can be approximated as  $\mathbf{E}^{\text{Biot}} \approx \mathbf{U} - \mathbf{I} = \mathbf{F} - \mathbf{I}$ , where  $\mathbf{U}$  is the unitary matrix from the polar decomposition of  $\mathbf{F}$  and  $\mathbf{I}$  is the unit matrix in  $\mathbf{R}^2$ . It is worthy to note, that with this simplification the strain energy associated with the stresses in Eqs. (8) and (9) fulfill material objectivity.

### 3. Experimental

#### 3.1. Experimental arrangements

To get proper parameters for the new constitutive law three experiment series were carried out: 5 pcs. uniaxial tensile tests both in the warp and the weft directions and 5 pcs. biaxial tests. To record data, a Messphysik ME-46 full image video-extensometer were used in all cases. The measured area was a 30×30 mm square in the middle of the specimen. The longitudinal and the transversal elongations were measured in all cases. The material of all the specimen was woven glass fiber with PTFE coating: Verseidag Duraskin B 18089 (Fig. 7.). The average thickness was 0.67 mm with a negligible variance, the surface density was 1150 g/mm<sup>2</sup>.

For the uniaxial test strip specimens were used: their width was 50 mm, the grip distance was 200 mm. Displacement test were carried out with tensile test machine Zwick Z020, the speed of elongation was 0.50 mm/s in all tests. The tests terminated after the failure (break) of the specimen and 40% of the ultimate load was used for parameter identification.

For the biaxial tests a special equipment was used with fixed ratio of the force in the two directions. It is a kind of pulley system developed by the authors (Bakonyi

et al. 2015, Hegyi 2016). The testing configuration can be seen in Fig. 8. An X shape specimen is folded through a pulley system: two “legs” are going up and two going down to the grips of a standard unidirectional tension testing machine. This system is not a universal tool to measure any ratios of forces in the two direction, however it is a simple extension of the uniaxial tensile procedure. The pulleys' position determines a flat area for the proper measurement. The width of the “legs” are 100 mm, the radius at the intersections are 25 mm. Displacement test were carried out, the speed was 0.80 mm/s in all tests.

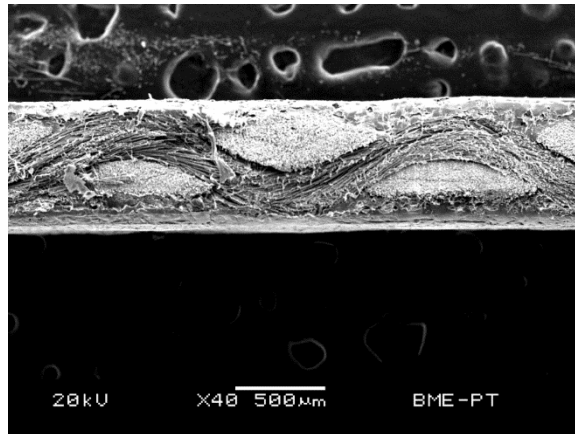


Figure 7. Microscopic photo of the section, the cut is parallel to the weft direction.

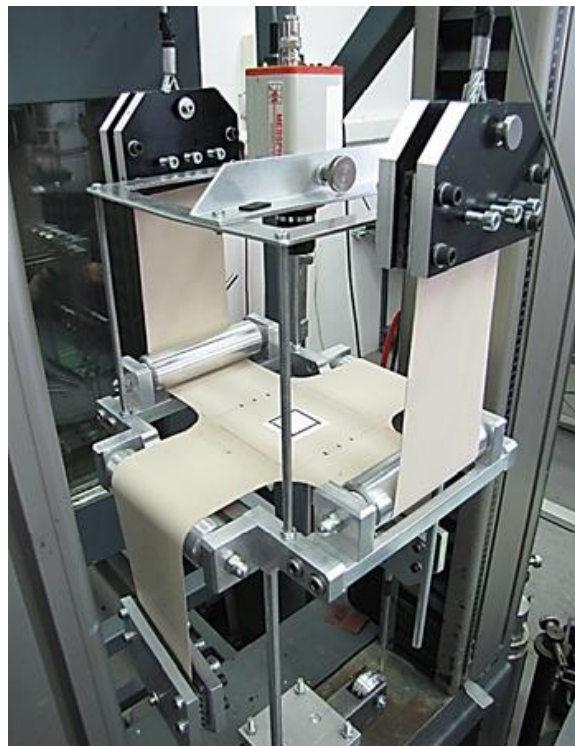


Figure 8. The bidirectional testing equipment.

The engineering stress in the optically measured area can be calculated as an average in case of the unidirectional test: the measured force of the testing machine is divided by the width of the specimen. To approximate the stress for the bidirectional tests a FEM analysis was needed. Unit stress were applied at the end of the “legs” of the virtual specimen. The stress level varies between 68.2-68.8% of the unit at the edge of the measuring area (Fig. 9), so it is almost

constant. Although it was a linear FEM analysis, we can expect almost the same distribution for the real specimen. From the measured force stress can be calculated to the “legs” of the specimen and the 68.5% of this stress were taken into account the measured area.

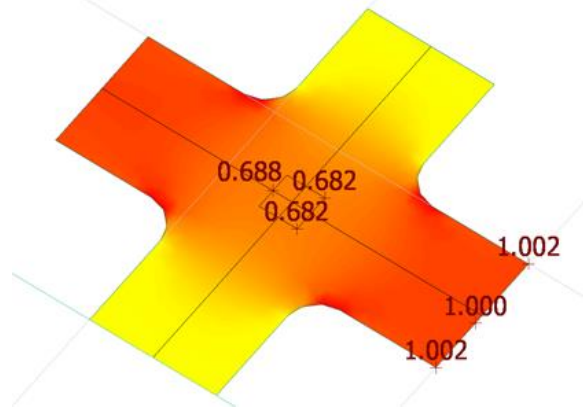


Figure 9. FEM analysis to approximate the stress level in the measured area.

### 3.2. Parameter identification

As it is general in the literature, the material parameters of the model might be approximated by a least square minimization from the measured data:

$$\Omega = \sum_{i=1}^n \left[ \left( s_{w,i} - \sigma_w(\varepsilon_{w,i}, \varepsilon_{w,i}) \right)^2 + \left( s_{f,i} - \sigma_f(\varepsilon_{w,i}, \varepsilon_{w,i}) \right)^2 \right] \Rightarrow \min \quad (11)$$

where  $n$  is the number of available measurements and  $s_{w,i}$  and  $s_{f,i}$  denote the measured stresses in the warp and weft directions, respectively. The objective function  $\Omega$  is the linear combination of the squared errors in the two directions. A serious shortcoming of such an approach is that due to the presence of the exponentials in the model (and the numerous material parameters) the objective function is far from being convex, it possesses many local minima. Even a slight change of the initial guess of the parameters can result in a significant shift in the parameter space. This is a widely known problem of regression models with exponentials (Golub and Pereyra 2003).

To obtain a reliable method, observe, that the following rearrangement of Eqs. (8) and (9) makes the third, interaction term vanish:

$$S := \sigma_w \varepsilon_w - \sigma_f \varepsilon_f = a_1 \varepsilon_w^2 (1 - e^{-a_3 \varepsilon_w^2}) + a_2 \varepsilon_w^2 (e^{-a_4 \varepsilon_w^2}) - b_1 \varepsilon_f^2 (1 - e^{-b_3 \varepsilon_f^2}) + b_2 \varepsilon_f^2 (e^{-b_4 \varepsilon_f^2}) \quad (12)$$

Nevertheless, a counterpart of  $S$ , namely  $T := s_w e_w - s_f e_f$  can be computed from the measured stress ( $s_w$  and  $s_f$ ) and strain data. To find the minimal deviation between  $S$  and  $T$  we use a MATLAB implementation of the variable projection method (O'Leary and Rust 2013). It determines all the linear and nonlinear parameters of the exponentials (i.e.  $a_1$ - $a_4$  and  $b_1$ - $b_4$ ) in our model. The range of plausible parameter values are summarized in Table 1. In numerical simulations,

we found, that this approach is much more robust for our data sets than a direct application of the least-square method in Eq. (11).

Table 1. Range of plausible parameter values of the model

	min	max
linear parameters: $a_1, a_2, b_1, b_2$	0	20
nonlinear parameters: $a_3, a_4, b_3, b_4$	0	5
interaction parameter: $c_1$	-5	5
interaction parameter: $c_2$	0	1

Having optimal values for the parameters of the exponentials we finally determine the parameters  $c_1$  and  $c_2$  in the interaction term. Here least-squares is a perfect choice: we substitute the already computed values of  $a_1$ - $a_4$  and  $b_1$ - $b_4$  into our model and apply Eq. (11) to obtain optimal values for  $c_1$  and  $c_2$ .

Note, that we expect positive reals for all parameters and in advance we expect  $c_2 < 1$  to match our observations about the transversal behavior (Fig. 4 and 5). Our scheme produces parameters in accordance with these expectations.

The best-fit parameters for the material in our experiments are:  $a_1=7.11, a_2=6.97, a_3=0.831, a_4=1.94, b_1=1.51, b_2=3.07, b_3=0.268, b_4=0.727, c_1=0.537, c_2=0.335$ . It is worthy to note that the applied methodology is fairly robust: parameter fit just for the uniaxial or solely for the biaxial data result in close parameter values to the ones presented above. The results of the parameter fit are represented in Figs. 10, 11, 12 and 13. Figs. 10 and 11 represent the stress by the function of both strain and the measured data are from uniaxial and biaxial tests. Figs. 12 and 13 represent the stress in the warp or the weft direction by the function of the warp or the weft strain respectively, uniaxial measures are on these plots.

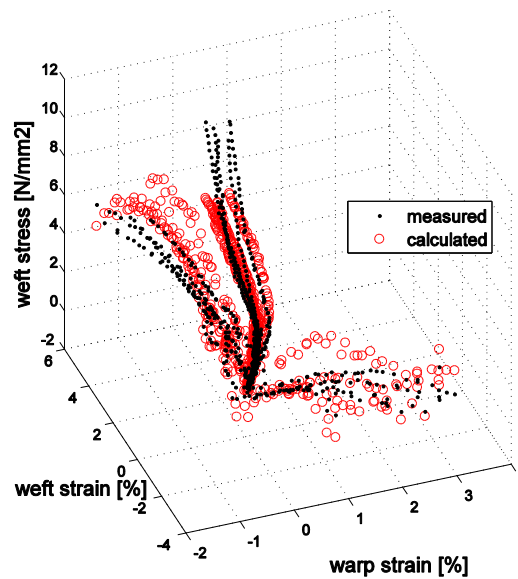


Figure 10. The general result of the parameter identification for the weft direction.

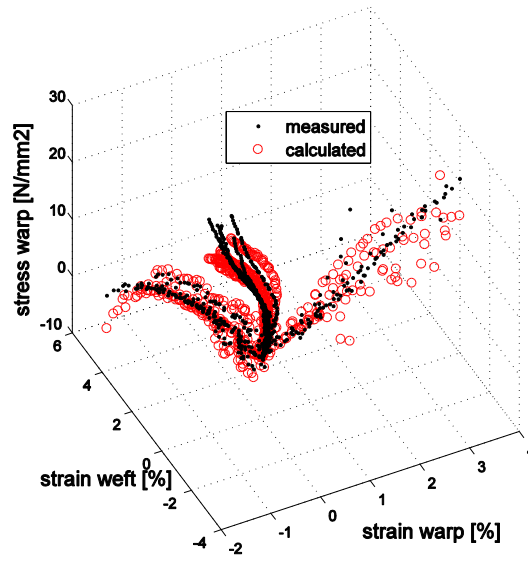


Figure 11. The general result of the parameter identification for the warp direction.

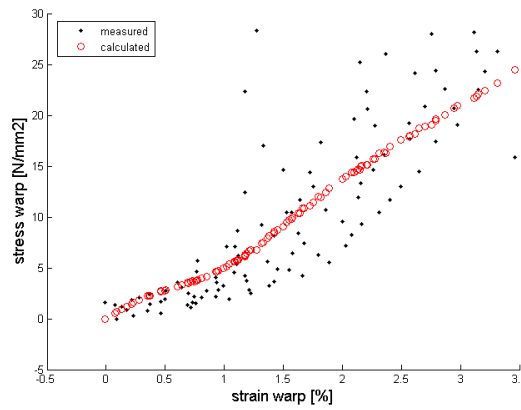


Figure 12. The uniaxial result of the parameter identification for the warp direction.

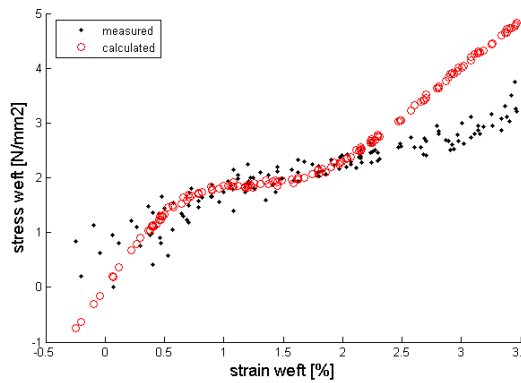


Figure 13. The uniaxial result of the parameter identification for the weft direction.

## 5. Discussion and verification

To obtain the actual normal stresses from the bidirectional strains Eqs. (8) and (9) are applied. In practical numerical analysis of a structure the constitutive law is

represented via the stiffness or the flexural matrices. A nonlinear constitutive law requires a nonlinear structural analysis. There are different strategies for nonlinear structures, for membrane structures the Total Lagrange Method (TLM) or the Updated Lagrange Method (ULM) can be regarded as typical.

In the case of TLM the deformation is calculated between the un-deformed, stress free state and the actual state. The secant of the stress-strain curve can be used:

$$D = \begin{bmatrix} \frac{\sigma_w}{\varepsilon_w} & \frac{\sigma_f}{\varepsilon_w} & 0 \\ \frac{\sigma_f}{\varepsilon_w} & \frac{\sigma_f}{\varepsilon_f} & 0 \\ 0 & 0 & G \end{bmatrix} > 0. \quad (13)$$

In the case of ULM the tangential stiffness matrix can be used:

$$D = \begin{bmatrix} \frac{\partial \sigma_w}{\partial \varepsilon_w} & \frac{\partial \sigma_f}{\partial \varepsilon_w} & 0 \\ \frac{\partial \sigma_f}{\partial \varepsilon_w} & \frac{\partial \sigma_f}{\partial \varepsilon_f} & 0 \\ 0 & 0 & G \end{bmatrix} > 0. \quad (14)$$

According to chapter 2.2  $G=(a_1+b_1)/(2 \times 100)=(7.11+1,51)/(2 \times 100)=0,043$  N/mm<sup>2</sup> is used for further analysis.

Another important criteria for a stable constitutive material law to have a positive definite stiffness matrix:

$$|D| = \begin{vmatrix} D_{ww} & D_{wf} & 0 \\ D_{wf} & D_{ff} & 0 \\ 0 & 0 & G \end{vmatrix} = \begin{vmatrix} \frac{\partial \sigma_w}{\partial \varepsilon_w} & \frac{\partial \sigma_f}{\partial \varepsilon_w} & 0 \\ \frac{\partial \sigma_f}{\partial \varepsilon_w} & \frac{\partial \sigma_f}{\partial \varepsilon_f} & 0 \\ 0 & 0 & G \end{vmatrix} > 0, \quad (15)$$

where  $D$  is the stiffness matrix of the material,  $D_{ww}$ ,  $D_{ff}$ ,  $D_{wf}$  and  $G$  are the members of the stiffness matrix for normal stress, transversal effect and shear, respectively.  $G$  is a positive, so for positive definiteness it is enough to prove:

$$D' = \frac{\partial \sigma_w}{\partial \varepsilon_w} \frac{\partial \sigma_f}{\partial \varepsilon_f} - \left( \frac{\partial \sigma_f}{\partial \varepsilon_w} \right)^2 > 0. \quad (16)$$

With the identified parameters the  $D'$  function can be drawn as a two-variable function of the strains (Fig.14). The surface is above 0 for reasonable strains (the stress is represented in percent, and normally the strain is under 4-5% even in the ultimate load level). At larger strains and in moderate negative strain  $D'$  is negative. Fig. 15 shows the border of the positive region, the zone containing the origin is positive. To have a stable numerical analysis the determinant should be controlled, but there is no problem in reasonable strain levels.

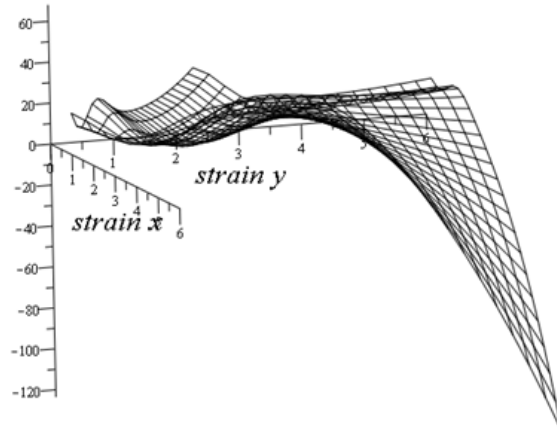


Figure 14. The surface of the  $D'$  function according to the strains.

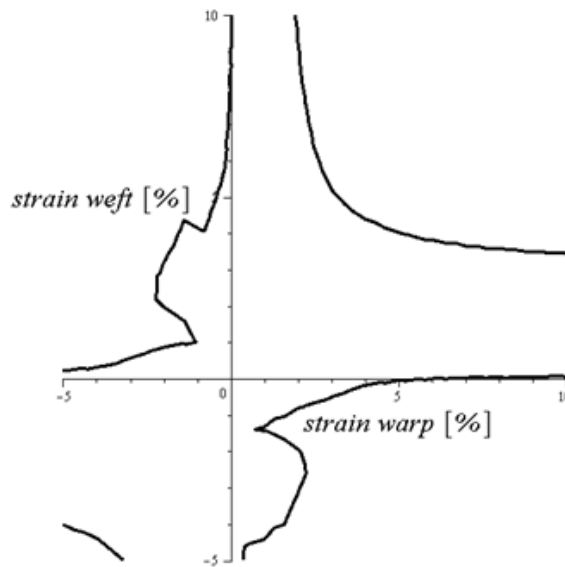


Figure 15. The intersection of the surface of the  $D'$  function with the 0 plan.

Fig. 15 shows, we are close to the border of the positive definite regime along the negative side of the axes, and over 5% of biaxial elongation. In classical Finite Element Method it can yield to instability, due to the requirement of the inverse of the stiffness. In any case for moderate strain the new constitutive model is stable. For extremely large strains the Dynamic Relaxation Method provides a proper strategy (Hegyi 2005, 2006). It does not use the inverse of the stiffness so positive definiteness is not an issue.

Both the power function methods (for instance the spline method) and the exponential functions we use have disadvantages at large strain. The benefit of the exponential approach introduced in this paper is the solid convergence to a slope instead of the hectic behavior of the power functions in extrapolation. In further work the model can be extended by a phenomenological damage model to explain the significant difference between the first loading and the cyclic behavior.

## 6. Conclusion

A new, elastic constitutive law for predicting service stresses of engineering textiles is introduced accompanied with a data acquiring strategy from uniaxial

and biaxial tension tests. The constitutive law accounts for both the nonlinear behavior of the yarns and the geometric nonlinearity of the fabric. Exponential functions are used to avoid the divergence of the numerical scheme in the nonlinear structural analysis. The new constitutive law fulfills all the requirements for a real material: existence of a strain energy function, positive definiteness at reasonable strain levels.

## Acknowledgements

The paper was supported by the János Bolyai Research Scholarship of the Hungarian Academy of Sciences [SA]

## References:

- Ambroziak, A., Klosowski, P.: Mechanical properties of polyvinyl chloride-coated fabric under cyclic tests. *Journal of Reinforced Plastics and Composites* **33**(3), 225–234. (2014)
- Ambroziak, A., Klosowski, P.: Nonlinear elastic and rheological constitutive modeling of PVC-coated polyester fabric using dense net model. In: *Proceedings of Structural Membranes 2005*, Stuttgart, 131–138. (2005)
- Bakonyi, P., Halász, M., Molnár, K., Szabó, D., Füzesi, T., Hegyi, D.: Development of a Biaxial Tensile Grip for Cyclic Tensile Tests of Flexible Technical Textiles. In: *Proceedings of 5th Edition of the International Conference on Intelligent Textiles & Mass Customization*, Casablanca 2015, (2015)
- Ballhause, D., König, M., Kröplin, B.: A microstructure model for fabric-reinforced membranes based on discrete element modeling. In: *Proceedings of Structural Membranes 2005*, Stuttgart, 255–264. (2005)
- Bodner, S. R., Partom, Y.: Constitutive equations for elastic-viscoelastic strain-hardening materials. *Journal of Applied Mechanics ASME* **42**, 385–389. (1975)
- Bridgens, B., Gosling, P. G.: Direct stress-strain representation for coated woven fabrics. *Computers and Structures* **82**, 1913–1923. (2004)
- Bridgens, B., Gosling, P. G.: A predictive fabric model for membrane structure design. In: *Proceedings of Structural Membranes 2005*, Stuttgart, 287–296. (2005)
- Chaboche, J. L.: Constitutive equation for cyclic plasticity and cyclic viscoelasticity. *International Journal of Plasticity* **5**, 247–302. (1989)
- Day, A. S.: Stress-strain equations for nonlinear behavior of coated woven fabrics. In: *IASS Symposium proceedings: shells, membranes and space frames*, Osaka, 2., 17–24. (1986)
- Durville, D.: Approach of the constitutive material behavior of textile composites through simulation. In: *Proceedings of Structural Membranes 2005*, Stuttgart, 307–316. (2005)
- Golub G. H., Pereyra, V.: Separable nonlinear least squares: the variable projection method and its applications. *Inverse Problems* **19**, R1–R26. (2003)
- Haan S. I., Charalambides P. G., Suri M.: A specialized finite element for the study of woven composites. *Computational Mechanics* **27**, 445–462. (2001)
- Hegyi, D., Sajtos, I., Geiszter, Gy., Hincz, K.: 8-node quadrilateral double-curved surface element for membrane analysis. *Computers and Structures* **84**, 2151–2158. (2006)
- Hegyi, D.: The analysis of membrane structures and structural membranes by numerical and experimental methods (in Hungarian). PhD Thesis (2006)
- dell'Isola, F., Steigmann, D.: A Two-Dimensional Gradient-Elasticity Theory for Woven Fabrics, *J. Elast.* 118:113-125. doi: 10.1007/s10659-014-9478-1 (2015)
- Lempriere, B.M.: Poisson's ratio in orthotropic materials. *AIAA Journal* **6**(11), 2226–2227. (1968)
- Sadd, M. H.: *Elasticity. Theory, Applications and Numerics*. Second Ed. Elsevier. (2009)
- Sipos, A. A., Fehér, E.: Disappearance of stretch-induced wrinkles of thin sheets: A study of orthotropic films. *Int. J. Solids&Struct.* 97–98: 275-283. doi: 10.1016/j.ijsolstr.2016.07.021. (2016)
- O'Leary, D. P., Rust, B. W.: Variable Projection for Nonlinear Least Squares Problems. *Computational Optimization and Applications*, 54:579 doi 10.1007/s10589-012-9492-9. (2013)